

Electronic Supplementary Information (ESI)

Tuning Chain Extenders Structure to Prepare High-Performance Thermoplastic Polyurethane Elastomers

Wei Juan Xu^a, Jian Jun Wang^{*a}, Shi Yu Zhang^a, Jun Sun^a, Chuan Xiang Qin^a, Li Xing Dai^a,
and Jia Jia Chen^b

^a College of Chemistry, Chemical Engineering and Materials, Science of Soochow University, Suzhou 215123, China

^b WestCHEM, School of Chemistry, the University of Glasgow, University Avenue, Glasgow G12 8QQ, Scotland (UK)

*Corresponding author. E-mail: wangjianjun@suda.edu.cn (Jian Jun Wang); Tel: 13915538961.

Table of contents:

1. Supplementary Table (Table S1)
2. Supplementary Figures (Fig. S1–S10)

1. Supplementary Table

Table S1 Comparison of thermal stabilities and mechanical properties of BDO-PU, monoFc-PU, and bisFc-PU.

| Samples | $T_{5\%}$ (°C) | T_{\max} (°C) | \bar{E}_a (KJ/mol) | Young's modulus (MPa) | Stress, σ_{\max} (MPa) | Strain, ϵ_{\max} (%) | Toughness (GJ m ⁻³) |
|-----------|-------------------|--------------------|-------------------------|-----------------------------|----------------------------------|----------------------------------|------------------------------------|
| BDO-PU | 298 | 300 | 110.6 | 7.3 | 27.5 | 932 | 10.6 |
| monoFc-PU | 321 | 350 | / | 6.0 | 6.0 | 758 | 2.4 |
| bisFc-PU | 345 | 369 | 214.9 | 13.9 | 42.3 | 1018 | 19.6 |

2. Supplementary Figures

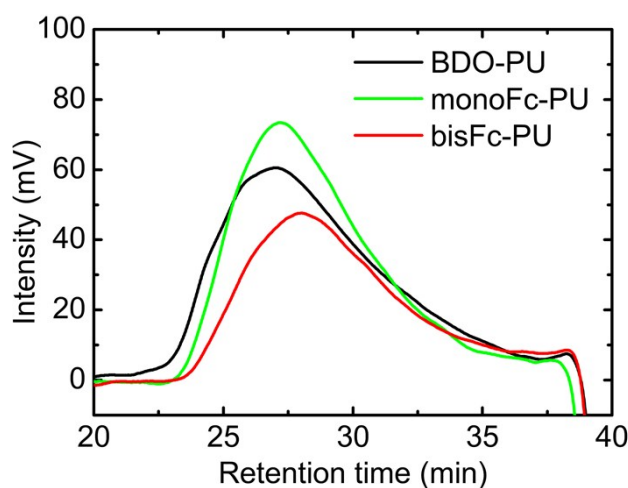


Fig. S1 Gel permeation chromatograph curves of BDO-PU, monoFc-PU and bisFc-PU were performed on a Waters-1515 using DMF-*LiBr* as an eluent and polystyrene (PS) as standards, the sample concentration was 2 ~ 3 mg mL⁻¹, and the flow rate was 0.800 mL min⁻¹ at 40 °C. The BDO-PU ($M_n = 3.6 \times 10^4$ g/mol, $M_w/M_n = 2.0$), monoFc-PU ($M_n = 3.0 \times 10^4$ g/mol, $M_w/M_n = 1.6$), and bisFc-PU ($M_n = 2.9 \times 10^4$ g/mol, $M_w/M_n = 1.5$).

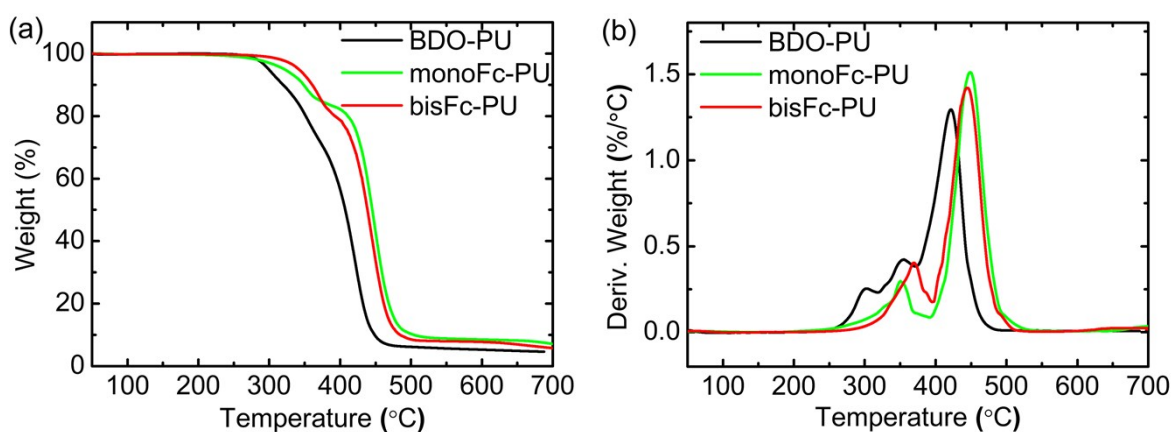


Fig. S2 (a) TGA and (b) DTG thermograms of- BDO-PU, monoFc-PU and bisFc-PU, at the heating rate of $10\text{ }^{\circ}\text{C min}^{-1}$ from 50 to 700 $^{\circ}\text{C}$ under nitrogen atmosphere.

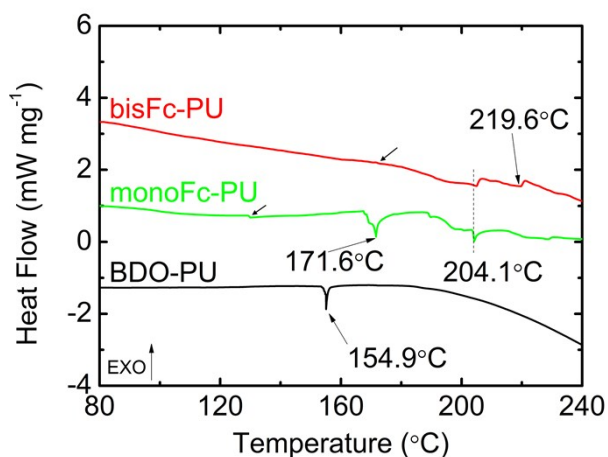


Fig. S3 The thermal behaviors of hard segments for BDO-PU, monoFc-PU and bisFc-PU. The curves were derived from differential scanning calorimeter (DSC) of the second heating processes between 80 to 240 $^{\circ}\text{C}$.

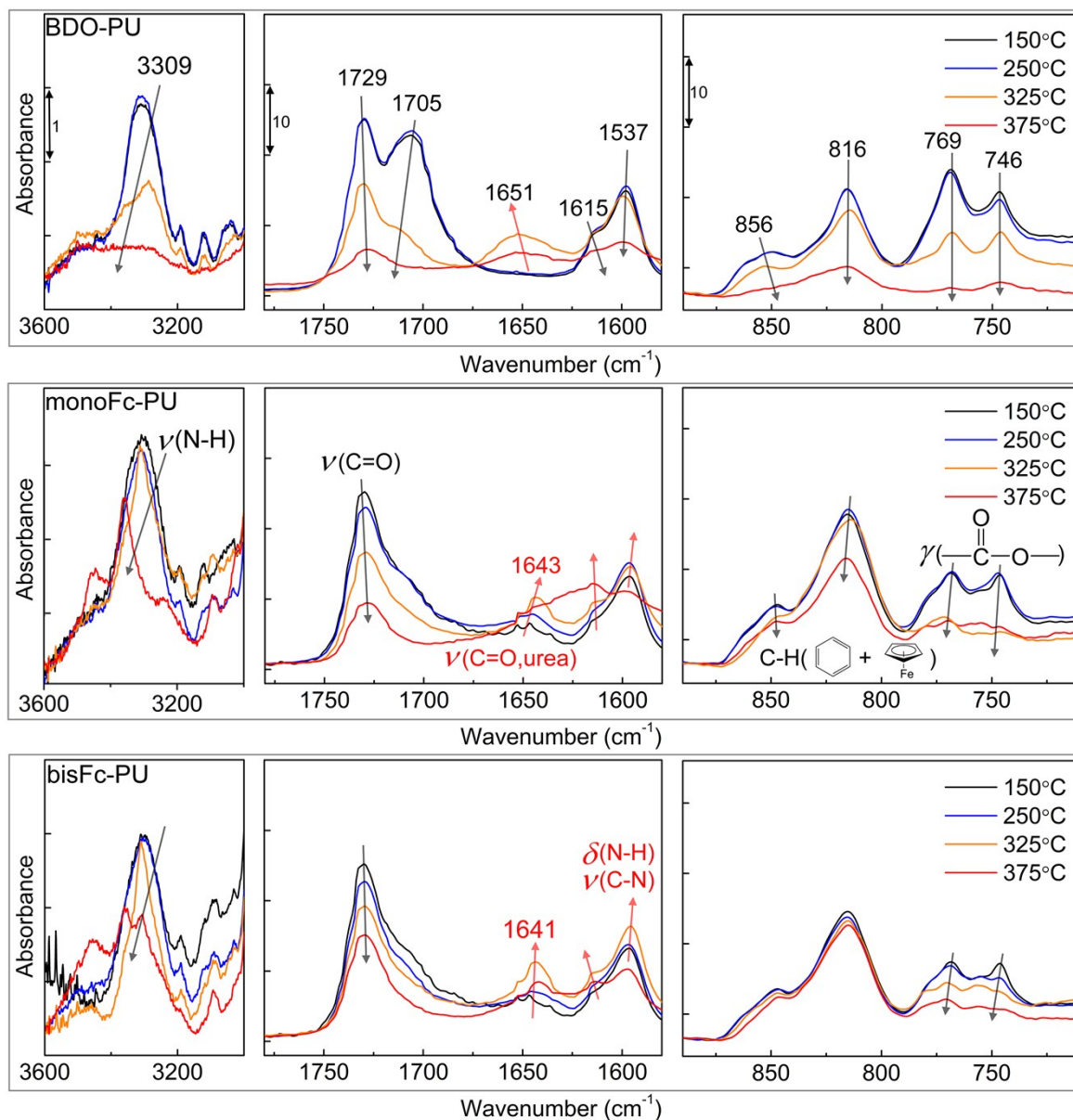


Fig. S4 Fourier transform attenuated total reflection infrared spectroscopy (ATR-FTIR) spectra at various temperature (150, 250, 325, 375 °C) of BDO-PU, monoFc-PU and bisFc-PU at the region of 3600 – 3000 cm^{-1} , 1780 - 1580 cm^{-1} and 890 - 700 cm^{-1} .

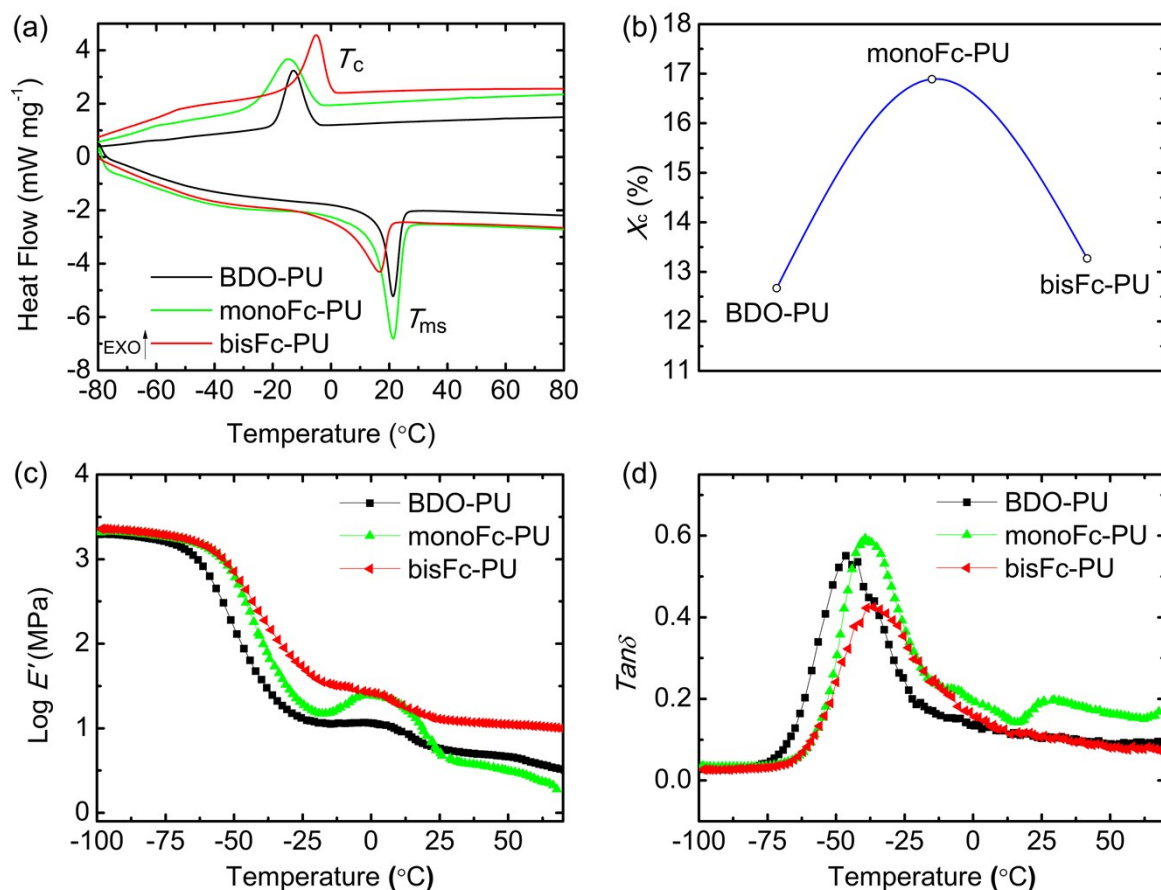


Fig. S5 (a) Differential scanning calorimeter (DSC) curves of first cooling and second heating processes and (b) The crystallinity (X_c) for BDO-PU, monoFc-PU and bisFc-PU; Dynamic mechanical analysis to show (c) the storage modulus and (d) $\tan \delta$ of BDO-PU, monoFc-PU and bisFc-PU from at a heating rate at 3 °C min⁻¹ from -100 to 80 °C. The degree of crystallinity (X_c) for those PUs were calculated via the equation of $X_c = \Delta H / \Delta H_0$, where ΔH is the heat fusion of PUs and ΔH_0 is the enthalpy of fusion of the fully crystalline material of $\Delta H_0 = 172.2 \text{ J g}^{-1}$.³¹

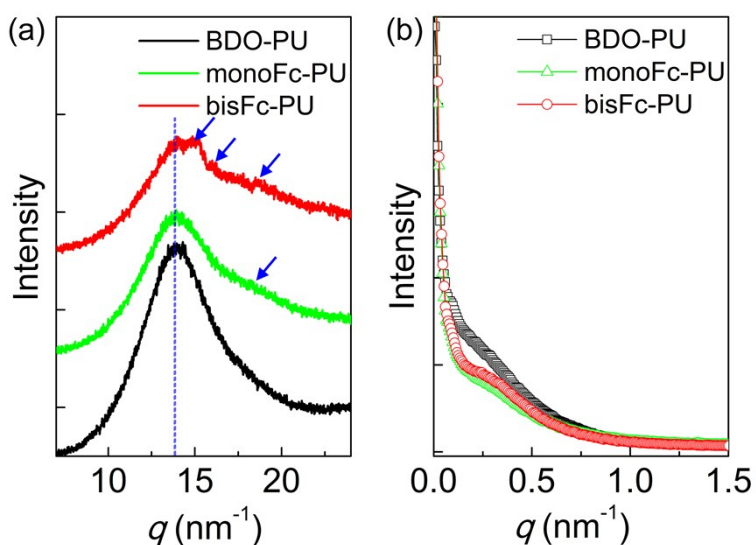


Fig. S6 (a) WAXD and (b) SAXS profiles of BDO-PU, monoFc-PU and bisFc-PU.

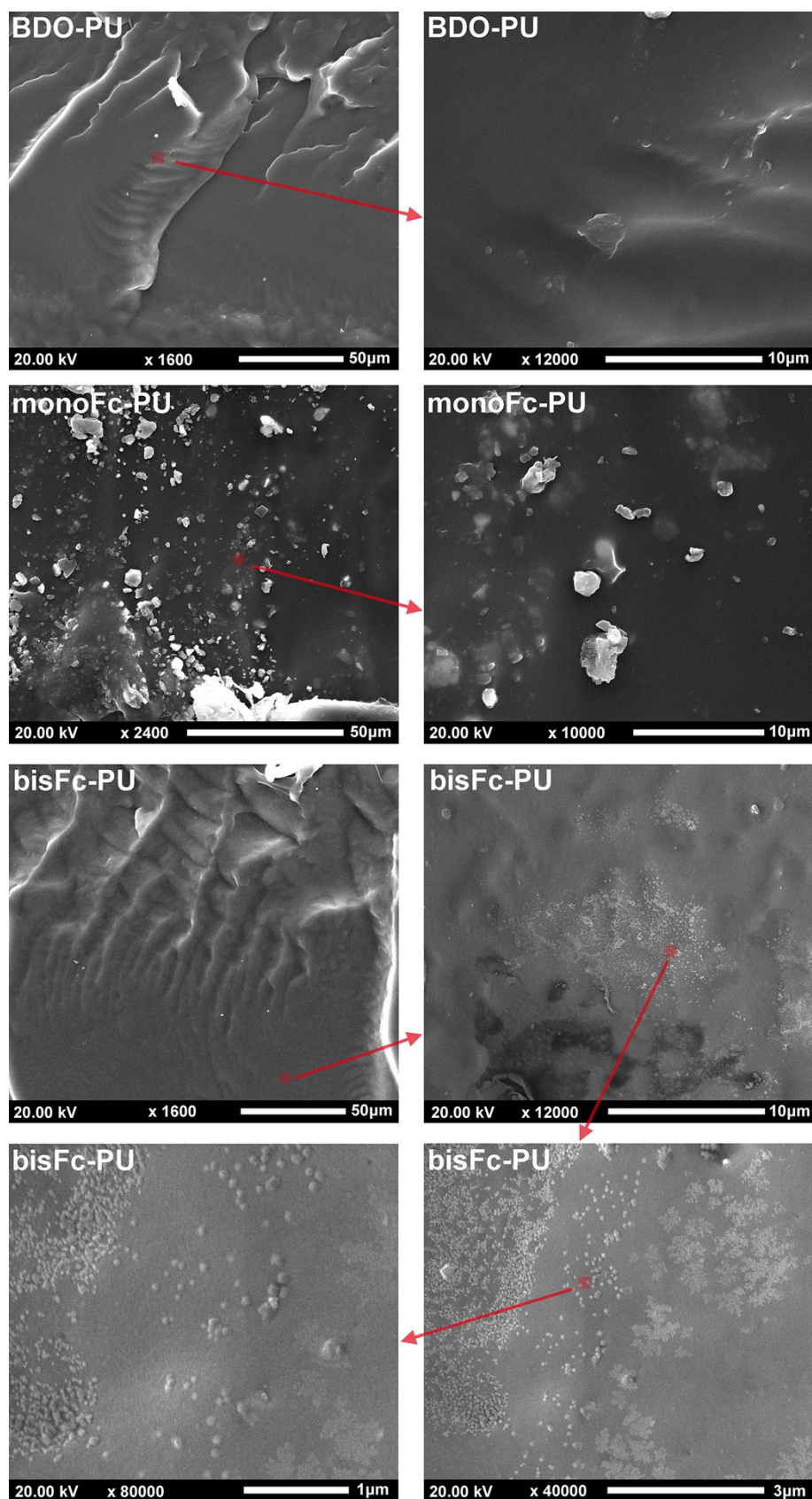


Fig. S7 SEM images of BDO-PU, monoFc-PU and bisFc-PU, and partial enlargements of the marked positions.

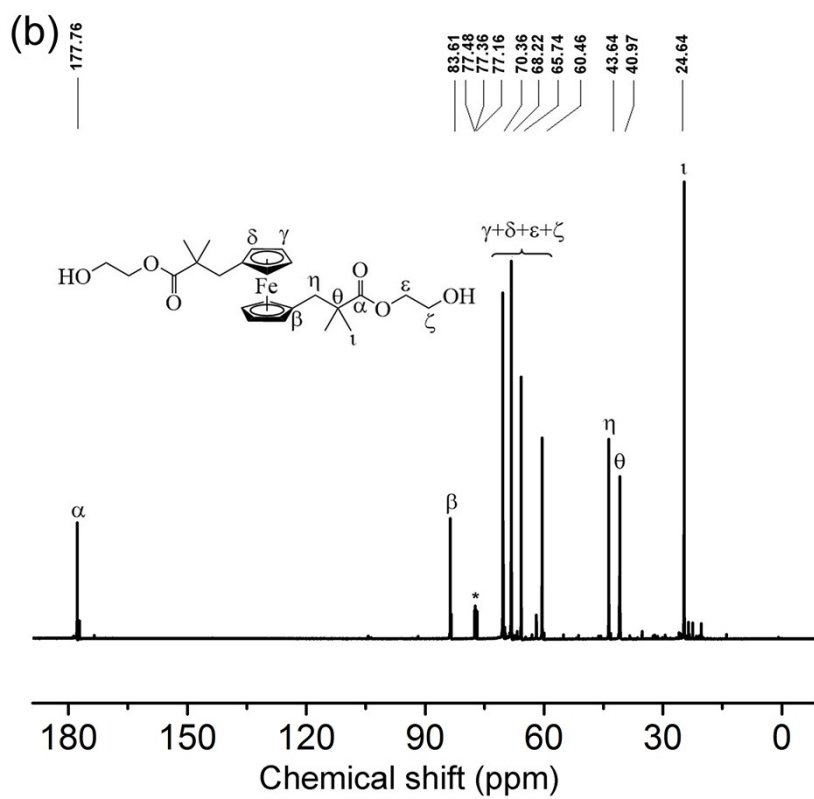
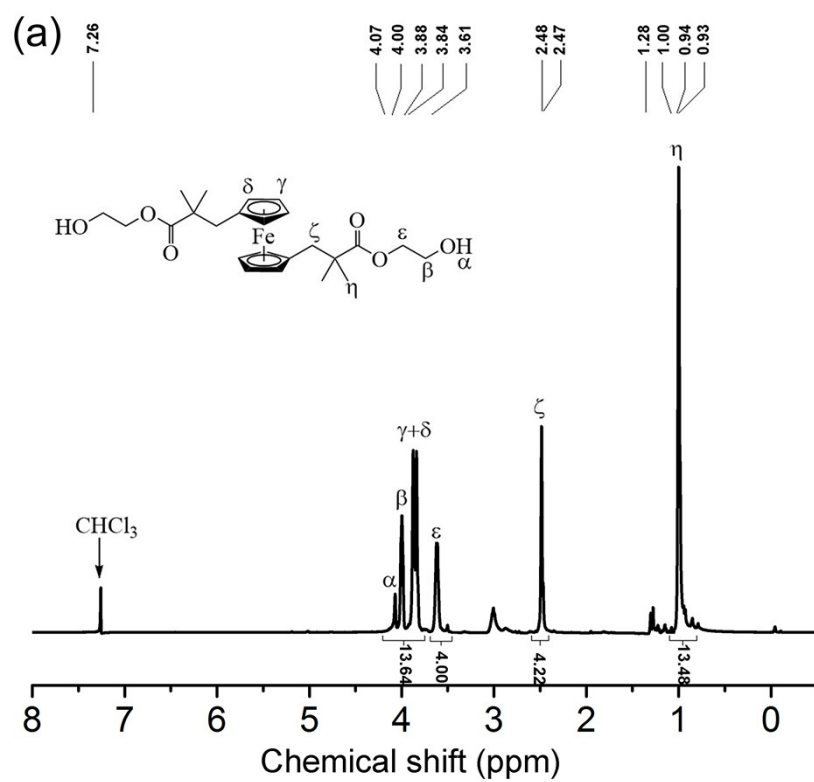


Fig. S8 (a) ^1H -NMR and (b) ^{13}C -NMR spectra for monoFc (600 Hz, CDCl_3).

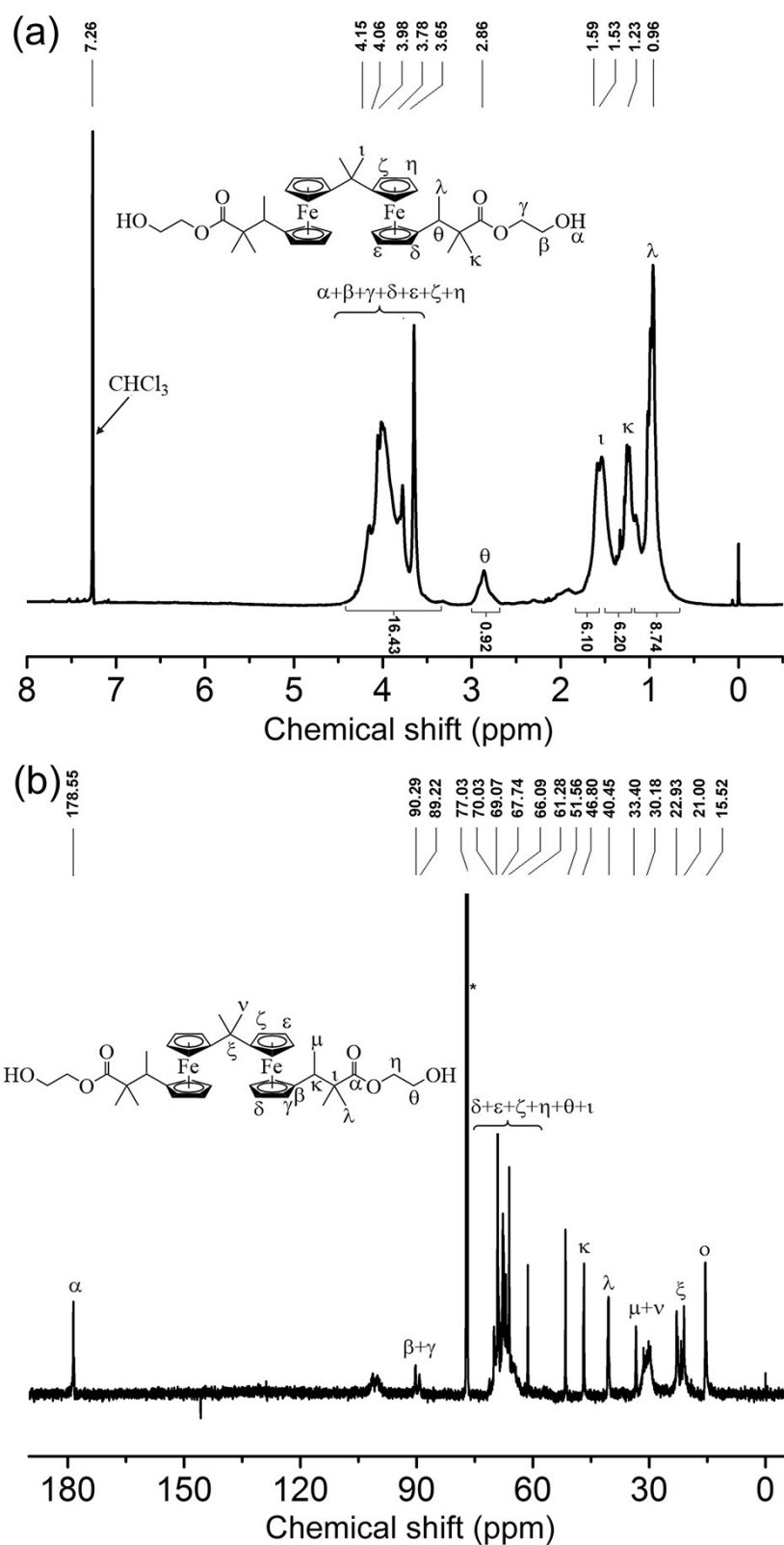


Fig. S9 (a) ¹H-NMR and (b) ¹³C-NMR spectra for bisFc (600 Hz, CDCl₃).

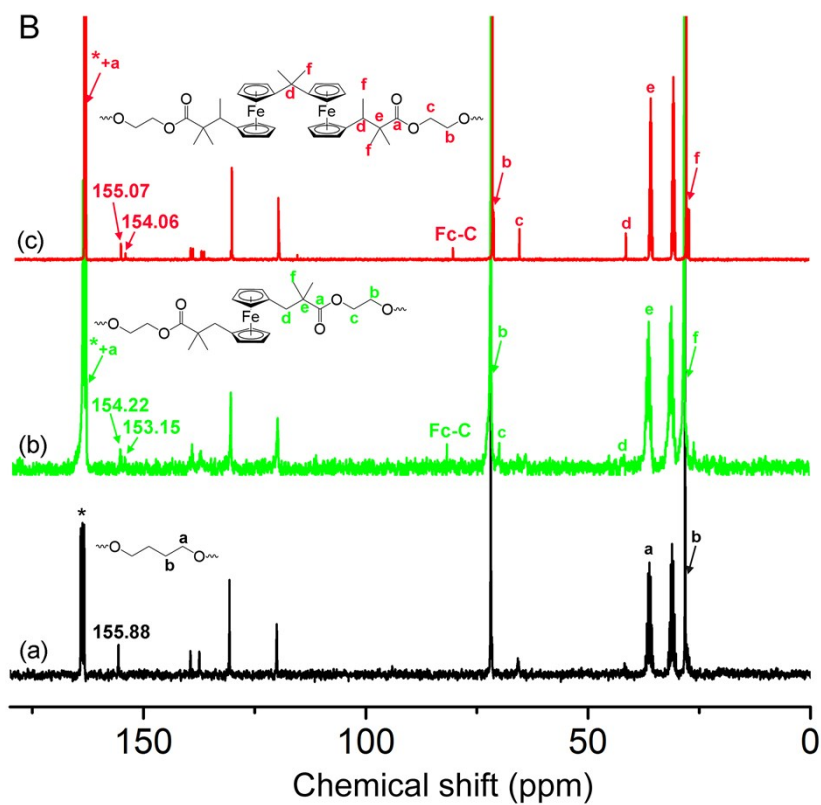
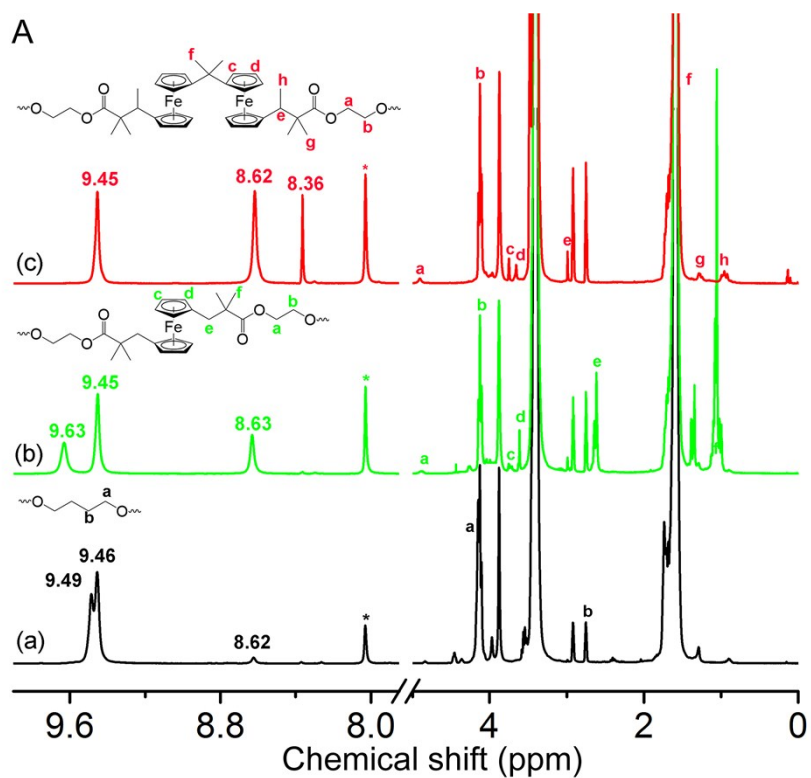


Fig. S10 A) ^1H -NMR and B) ^{13}C -NMR spectra for (a) BDO-PU, (b) monoFc-PU, and (c) bisFc-PU (600 Hz, $\text{DMF-}d_7$). (*) Signals of solvent.